Redox Biology 78 (2024) 103422

Contents lists available at ScienceDirect

Redox Biology

journal homepage: www.elsevier.com/locate/redox

Time-restricted eating reveals a "younger" immune system and reshapes the intestinal microbiome in human

Yiran Chen [a,b,c,d,1], Xi Li [e,1], Ming Yang [e,1], Chen Jia [e], Zhenghao He [e], Suqing Zhou [e], Pinglang Ruan [e], Yikun Wang [f], Congli Tang [g], Wenjing Pan [g,h], Hai Long [e], Ming Zhao [a,e], Liwei Lu [i], Weijun Peng [j], Arne Akbar [k], Irene XY. Wu [l], Song Li [m,n,***], Haijing Wu [e,**], Qianjin Lu [a,b,c,d,e,*]

[a] Hospital for Skin Diseases, Institute of Dermatology, Chinese Academy of Medical Sciences & Peking Union Medical College, Nanjing, 210042, China
[b] Key Laboratory of Basic and Translational Research on Immune-Mediated Skin Diseases, Chinese Academy of Medical Sciences, Nanjing, 210042, China
[c] Jiangsu Key Laboratory of Molecular Biology for Skin Diseases and STIs, Nanjing, 210042, China
[d] Research Unit of Key Technologies of Immune-related Skin Diseases Diagnosis and Treatment, Chinese Academy of Medical Sciences Institute of Dermatology, Nanjing, 210042, China
[e] Department of Dermatology, The Second Xiangya Hospital of Central South University, Hunan Key Laboratory of Medical Epigenomics, 139 Middle Renmin Road, Changsha, Hunan, 410011, China
[f] Department of Pharmacy, The Second Xiangya Hospital, Central South University, Changsha, 410011, China
[g] Nanjing ARP Biotechnology Co., Ltd, Nanjing, 210046, China
[h] Hunan Key Laboratory of Biomedical Nanomaterials and Devices, Hunan University of Technology, Zhuzhou, 412007, China
[i] Department of Pathology and Shenzhen Institute of Research and Innovation, The University of Hong Kong, Hong Kong, 518057, China
[j] Department of Integrated Traditional Chinese & Western Medicine, The Second Xiangya Hospital of Central South University, Changsha, Hunan, 410011, China
[k] Associate of the Institute of Healthy Ageing, Division of Infection & Immunity, University College of London, London, WC1E 6BT, United Kingdom
[l] Xiangya School of Public Health, Central South University, 4/F, Changsha, Hunan, 410006, China
[m] Key Laboratory of Rare Pediatric Diseases, Ministry of Education, Hengyang Medical School, University of South China, Hengyang, Hunan, China
[n] National Health Commission Key Laboratory of Birth Defect Research and Prevention, Hunan Provincial Maternal and Child Health Care Hospital, Changsha, Hunan, China

ARTICLE INFO

Keywords:
Time-restricted eating
Immune cellular senescence
Intestinal microbiome
Immune repertoires
Metabolomic
Young

ABSTRACT

Time-restricted eating (TRE) has been shown to extent lifespans in drosophila and mouse models by affecting metabolic and anti-inflammatory activities. However, the effect of TRE on the human immune system, especially on immunosenescence, intestinal microbiome, and metabolism remains unclear. We conducted a 30-day 16:8 TRE single-arm clinical trial with 49 participants. Participants consumed daily meals from 9 a.m. to 5 p.m., provided by a nutrition canteen with a balanced, calorie-appropriate nutrition, which is designed by clinical nutritionists (ChiCTR2200058137). We monitored weight changes and weight-related parameters and focused on changes in the frequency of $CD4^+$ senescent T cells, immune repertoire from peripheral blood, as well as serum metabolites and gut microbiota. We found that up to 95.9 % of subjects experienced sustained weight loss after TRE. The frequency of circulating senescent $CD4^+$ T cells was decreased, while the frequency of Th1, Treg, Tfh-like, and B cells was increased. Regarding the immune repertoire, the proportions of T cell receptor alpha and beta chains were increased, whereas B cell receptor kappa and lambda chains were reduced. In addition, a reduced class switch recombination from immunoglobulin M (IgM) to immunoglobulin A (IgA) was observed. TRE upregulated the levels of anti-inflammatory and anti-aging serum metabolites named sphingosine-1-phosphate and prostaglandin-1. Additionally, several anti-inflammatory bacteria and probiotics were increased, such as *Akkermansia* and *Rikenellaceae*, and the composition of the gut microbiota tended to be

* Corresponding author. Hospital for Skin Diseases, Institute of Dermatology, Chinese Academy of Medical Sciences & Peking Union Medical College, Nanjing, 210042, China.
** Corresponding author.
*** Corresponding author. Key Laboratory of Rare Pediatric Diseases, Ministry of Education, Hengyang Medical School, University of South China, Hengyang, Hunan, China.
E-mail addresses: sosong1980@gmail.com (S. Li), Chriswu1010@csu.edu.cn (H. Wu), qianlu5860@pumcderm.cams.cn (Q. Lu).
[1] These three authors contributed equally to this work.

https://doi.org/10.1016/j.redox.2024.103422
Received 10 October 2024; Received in revised form 31 October 2024; Accepted 5 November 2024
Available online 9 November 2024

"younger". Overall, TRE showed multiple anti-aging effects, which may help humans maintain a healthy lifestyle to stay "young". Clinical Trial Registration URL: https://www.chictr.org.cn/showproj.html?proj=159876.

1. Introduction

Obesity has been identified as one of the most prevalent chronic disease worldwide [1]. Multiple fundamental studies have revealed that obese people have low-grade, chronic inflammation [2], which contributes to the development of insulin resistance [3]. In addition, T cells in obesity-related visceral adipose tissue have been reported to undergo cellular senescence, potentially leading to accelerated immunosenescence [4]. Therefore, except for metabolism-related diseases, obesity may contribute to immunosenescence-related disorders.

To fight obesity, low-calorie diets and fasting have been proposed and have shown great effects on weight loss [5]. To our surprise, low-calorie diets and fasting regimens also relieve the clinical phenotypes of autoimmune and inflammatory diseases, including multiple sclerosis [5] and rheumatoid arthritis (RA) [6], and even extend the lifespan of mice [7]. Time-restricted eating (TRE) is a method of fasting that involves restricting daily food intake to a period of 6–8 h. TRE has been found to reduce blood glucose, body mass index and body fat, alleviate inflammation and increase the diversity of the gut microbiome [8]. Some studies have suggested that TRE provides benefits by

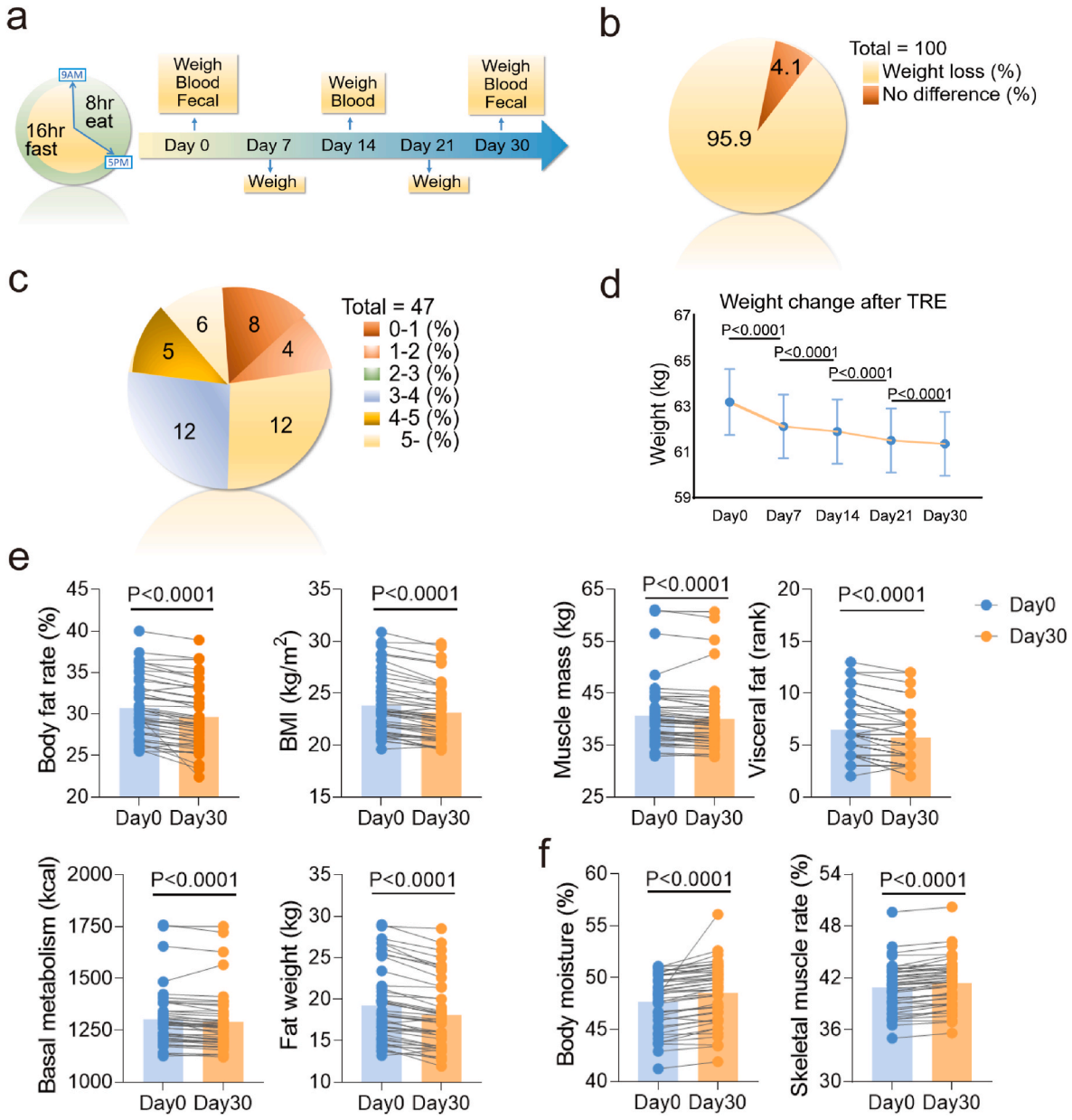

Fig. 1. Experimental design and changes in body weight and related indexes before and after TRE. (a) Eating window, sampling timeline and specimen collection during TRE; (b) Proportion of participants who experienced weight loss after 30 days of TRE; (c) Statistics of weight loss based on different percentage ranges; (d) Continued weight loss observed in participants during 30-day TRE. (e) Statistical analysis of the change of body fat rate, body mass index (BMI), muscle mass, body moisture, visceral fat, basal metabolism, fat weight and skeletal muscle rate before and after a 30-day TRE. n = 45. Statistical analysis was performed using Mauchly's Test of Sphericity in Fig. 1d and paired *t*-test at two different time points in Fig. 1e and f. Data are mean ± s.e.m in Fig. 1d.

enhancing the process of autophagy [9]. However, the effect of TRE in human immunosenescence remains unclear.

Senescence occurs in the aging status, and it also manifests in pathological conditions such as breast cancer [10,11], RA and acquired immune deficiency syndrome [12]. Cellular senescence refers to a state in which a cell exhibits cell cycle arrest, apoptosis resistance, cell dysfunction and secretion of senescence-associated secretory phenotypes (SASP), such as IL-6 and TNF-alpha. Immunosenescence involves inflammation and the accumulation of senescent cells [13]. Senescent immune cells, such as senescent T cells, play a crucial role in the development of age-related diseases [14], including cancer, atherosclerosis and osteoarthritis. Although previous studies have reported that fasting on alternate days regulates aging-related metabolism in healthy adults [15], it remains to be clarified how TRE affects immune system function and the immunosenescent state in humans. Therefore, we established a clinical trial, *Effect of Time-Restricted Eating on the Immune System (TREI),* in healthy subjects. This trial contributes to our better understanding of the benefits of TRE and may provide a candidate regimen for public health.

2. Results

2.1. Study design

This study was a single-arm clinical trial with a TRE group (n = 49) and a control group (n = 10). The consort flow diagram is shown in Fig. S1. Over a period of 30 consecutive days, the TRE participants consumed a balanced diet (Table S1) and were restricted to eating between 9 a.m. and 5 p.m. All TRE subjects completed the trial without loss to follow-up or poor completion. Fig. 1a illustrates the eating window, sampling timeline and specimen collection for the TRE group. The weight of TRE participants was recorded before the intervention, while their weight was recorded once a week during the dietary intervention. Peripheral blood was collected from TRE participants before the trial and at Day 0, Day 14 and Day 30 of the trial on their fasting state (8:00 a.m.), and samples of stool were collected before and after the trial. Day 90 after TRE ended, we reweighed participants and collected peripheral blood to observe the long-term effects of TRE. For the subjects in the control group, their diet structure was similar to that in the TRE group, and there was no intervention on food intake. Blood samples were collected and body weight and weight-related indicators were measured only on Day 0 and Day 30.

In the TRE group, we conducted the analysis of weight and weight-related indicators, circulating T and B cell frequencies, circulating $CD4^+$ senescent T cell frequencies, immune repertoire (IR) sequencing, liquid chromatography-mass spectrometry (LC-MS) metabolomic analysis and 16S rDNA microbiome sequencing. In the control group, data were analyzed from IR sequencing to body weight and weight-related indicators on Day 0 and 30 (Fig. S1). Besides, new evidence shows that immunological aging doesn't align with biological aging, with notable age turning points at 34, 60, and 78 [16]. In the Chinese population, pronounced changes in aging, metabolism, and immunity occur around age 30 [17,18]. Therefore, we divided participants into two subgroups: the under 30 years old TRE group (<30 y) and the over 30 years old TRE group (>30 y), to better understand TRE's impact on immunosenescence. In this study, we hypothesized that 16:8 TRE for 30 days in healthy participants would reduce the proportion of $CD4^+$ senescent T cells in peripheral blood.

2.2. TRE reduced body weight and weight-related indicators

95.9 % of TRE participants lost weight (Fig. 1b). Most of them lost 2–4% of their body weight (Fig. 1c). Weight losing among participants continued steadily throughout the 30-day TRE period (Fig. 1d). Meanwhile, changes were also observed in weight-related indicators before and after the 30-day TRE. The value of body fat rate, body mass index (BMI), muscle mass, visceral fat, basal metabolism and fat weight decreased significantly (Fig. 1e). On the other hand, the value of body moisture and skeletal muscle rate was increased significantly after a 30-day TRE (Fig. 1f).

According to previous studies, the aging-related and metabolism-related changes in Chinese people show a dramatic peak at the age of 30[17]. Interestingly, similar trends were observed in the age subgroup analysis of TRE (Figs. S2a and b). In order to exclude the influence of confounding factors such as seasons, live conditions, temperature change and diet pattern on body weight and weight-related indicators, we also recruited 10 healthy volunteers with similar living conditions (from the same research center), diet patterns to TRE group, without eating time restriction, and measured body weight and weight-related indicators on Day0 and Day30. There was no difference in body weight and weight-related indicators in this control group (Fig. S2c), indicating that the changes might be attributed to TRE.

2.3. TRE increased the proportion of circulating Th1, Tfh-like and Treg cells while reduced the proportion of circulating $CD8^+$ T cells

The TRE-induced changes in lymphocytes were investigated in 40 healthy participants by analyzing circulating T and B cell subsets on Day 0, Day 14, Day 30 of TRE and Day 90 after TRE ended. The identified markers of each cell subset are listed in Table 2.

Interestingly, after 30 days of TRE, the frequencies of lymphocytes in the participants were changed. The frequency of total $CD3^+$ T cells was decreased (Fig. S3a). The frequency of $CD3^+$ T cells decreased at Day 30 but increased to baseline levels after the end of TRE in the <30 y group (Fig. S4a). The frequency of total $CD4^+$ T cells remained stable during TRE (Fig. S3a, Fig. S4a). For the subsets of $CD4^+$ T cells, we found that the frequency of $CD4^+$ naive T cells was decreased while the frequency of $CD4^+$ effector T cells was higher than that on Day 0 (Fig. S3b), while no significant differences were observed in the age subgroup analysis (Fig. S4a). We further analyzed the effect of TRE on $CD4^+$ helper T cells. The frequency of Th1 cells increased, while Th2 cells and Th17 cells decreased after 30-day TRE (Fig. 2a). The frequency of Tfh-like cells and Treg cells increased on Day 30 and then decreased to baseline levels at Day 90 after the end of TRE (Fig. 2b). In addition, we found the changes in the frequencies of Th1, Th2, Th17, Tfh-like and Treg cells in different age group were in accordance with the general trend of the ungrouped results (Fig. S4b). The frequency of total $CD8^+$ T cells was decreased (Fig. S3a). For the subsets of $CD8^+$ T cells, the frequency of $CD45RA^+CD8^+$ T cells was decreased (Fig. S3c) and that of $CD45RA^-CD8^+$ T cells was increased after 30-day TRE (Fig. S3c). Fig. S4a shows the subgroup analysis of $CD8^+$ T lymphocytes based on age stratification at 30 years old. There were no significant differences in the changing trend of $CD8^+$ T lymphocyte frequencies between the two age subgroups during TRE.

2.4. TRE reduced the proportion of circulating senescent $CD4^+$ T cells

To evaluate the levels of immunosenescence, we further assessed the impact of TRE on circulating senescent $CD4^+$ T ($CD4^+CD27^-CD28^-$) cells. We found that the frequency of senescent cells in total $CD4^+$ T cells dramatically reduced during TRE (Day14, 30) and continuously decreased on Day 90 after TRE ending (Fig. 2c). Further, the frequency of senescent cells in total $CD4^+$ T cells in >30y group was higher than that in <30y group in baseline, as expected. Interestingly, the frequency of $CD4^+$ senescent T cells was reduced in both the >30y group and <30y group, and the downward trend was maintained 90 days after TRE in the >30y group (Fig. S4c).

2.5. TRE increased the proportion of circulating total B cells in healthy individuals

In addition, we observed that the frequency of total $CD19^+$ B cells

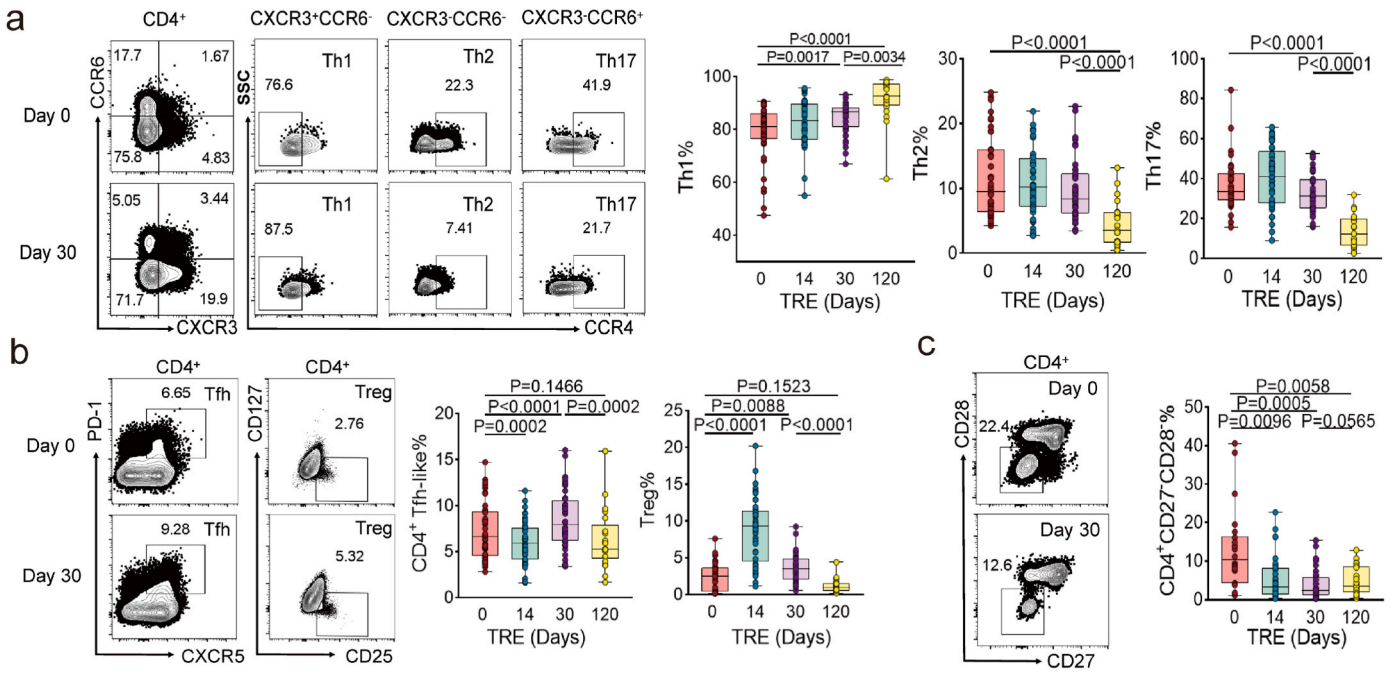

Fig. 2. Frequencies of $CD4^+$ T subsets from PBMCs before and after TRE.
Statistical analysis and cytometry gates of (a) $CD4^+Th_1$, Th2 and Th17 cells; (b) $CD4^+$Tfh-like and T_{reg} cells for each T-cell subset from PBMCs of the TRE Day 0 (n = 41), Day 14 (n = 41), Day 30 (n = 40) and Day 90 after TRE groups (n = 19). (c) Statistical analysis and cytometry gates of $CD4^+$ senescent cells ($CD27^-CD28^-$) in the TRE Day 0 (n = 22), Day 14 (n = 38), Day 30 (n = 37) and Day 90 after TRE groups (n = 21). Statistical analysis was performed using paired *t*-test at two different time points in Fig. 2a, b and c. Data are mean ± s.e.m.

increased continuously from Day 0 to Day 30 but dropped to baseline level at Day 90 after TRE (Fig. S3d). For the B-cell subsets, there were no significant changes in classical memory B cells or naive B cells. Meaningfully, the ratio of plasma cells (PCs) remained stable during TRE (Fig. S3d).

There was no difference in the frequency of total $CD19^+$ and classical memory B cells between age subgroups at baseline. However, the frequency of naive B cells was higher and plasma cells was lower in the >30y group at baseline. After conducting subgroup analysis by age, we observed the same change of total $CD19^+$ cells both in total and the two age subgroups (Fig. S5).

2.6. TRE increased the frequency of TCR alpha and beta chains and decreased BCR-kappa and lambda chains

T cell receptor (TCR) and B cell receptor (BCR) are essential elements of adaptive immunity and constitute IRs [19]. The diversity and distribution of immune receptor clones, reflecting clonal selection and expansion, can uniquely indicate an individual's immunological state (e.g., healthy, infected, vaccinated) and be utilized for immunodiagnostic purposes. IR sequencing was conducted before and after 30-day TRE to evaluate its effects on the immune system on multiple dimensions.

After 30-day TRE, the proportion of 7 chains in volunteer peripheral blood mononuclear cells (PBMCs) in the >30y TRE, <30y TRE and control groups changed apparently (Fig. 3a). Compared with Day 0, the percentage of TCR alpha chains and beta chains increased (Fig. 3b) and the percentage of BCR heavy chains among the seven sequenced chains declined (Fig. 3b). Moreover, these changes were predominantly observed in >30y group (Figs. S6a and b). Notably, there was no discernible difference in diversity (represented by d50) between TRE and its predecessors (Fig. S6c).

2.7. TRE decreased BCR large clones and reduced class switch recombination in PBMCs

The treemaps in Fig. 3c depict the seven-chain repertoire of typical participants before and after a 30-day TRE. In the treemaps, the area corresponds to the proportion of TCR alpha, beta, delta, gamma, BCR heavy, kappa and lambda chains, arranged from up to down and left to right. Larger color blocks indicate larger clones. The treemaps show the same changes in the proportions of the seven chains before and after TRE as in Fig. 3a and b and S6a and b. Besides, it can be observed that after 30 days of TRE, the four chains of TCR were compressed by the BCR chain, while the large clones of heavy, kappa and lambda BCR chains were significantly reduced, thus the distribution of TCR and BCR became more balanced after TRE.

Additionally, Fig. 3d revealed variations in the proportions of immunoglobulins among the six isotypes of BCR before and after intervention. After 30 days of TRE, the proportion of immunoglobulin A (IgA) decreased (Fig. S7a), especially in the >30 y group (Fig. S7b), while the proportion of immunoglobulin M (IgM) increased (Fig. S7a). However, there was no difference in serum secreted immunoglobulin levels both in the TRE group and the control group. Moreover, age subgroup analyses of the TRE group also did not show significant differences (Figs. S7c and d). In antigen-antibody immune responses, the mature naive B cells produce IgM and immunoglobulin D (IgD) and undergo the class switch recombination (CSR) to produce isotype-switched high-affinity antibody immunoglobulin G (IgG), IgA or immunoglobulin E (IgE) that can best protect against the pathogen [20,21]. CSR is generally considered a hallmark of germinal centers and it also occurs readily in extrafollicular responses [22]. Active CSR represents active immune response and the "CSR index" was utilized to quantify the immune response before and after 30 days of TRE [23]. The thickness of the arrow represents the percentage of CSR between the immunoglobulins (Igs). Fig. 3e shows a dramatic decrease in the CSR index values for the switch from IgM and IgD to IgG, IgE, or IgA expression after TRE, observed in both the <30 y

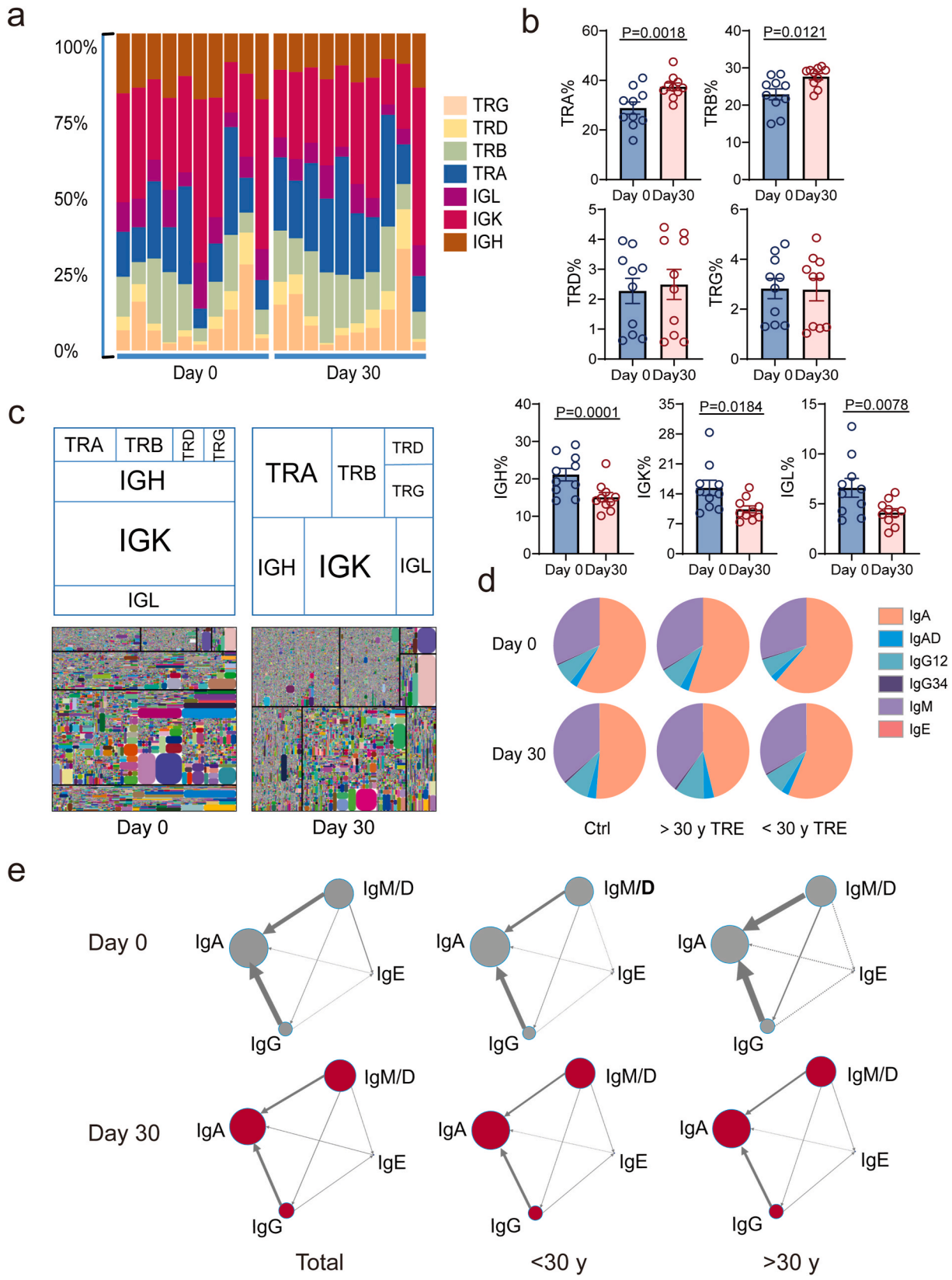

Fig. 3. Immune repertoire changes before and after 30 days of TRE. (a) Proportion of 7 chains in volunteer PBMCs before and after TRE by counting unique CDR3; (b) Statistical analysis of the percentage changes in the proportions of BCR and TCR chains across time points; (c) The representative treemaps showing the 7-chain repertoire in PBMCs before and after the 30-day TRE. (d) The proportion of the 5 Ig isotypes in >30 y TRE, <30 y TRE and Ctrl groups by counting reads; (e) The CSR index values of five Ig before and after the 30-day TRE for the >30 y TRE, <30 y TRE groups and in total. The arrow indicates the direction of class switching, and the thickness of the arrow connecting lines indicates the displacement of the CSR index. The spheres represent different Ig isotypes. The graph displays IgM and IgD as a whole. > 30 y TRE, n = 5, <30 y TRE, n = 5, Ctrl, n = 5. Statistical analysis was performed using a paired *t*-test shown in Fig. 3b. Data are mean ± s.e.m in Fig. 3b.

and >30 y groups. The decrease in CSR index values indicates TRE may reduce the activation ability of B cells.

2.8. TRE attenuated serum inflammation by altering the abundance of inflammation-related metabolites

Considering the lack of changes in weight and immune system in the control group, the serum metabolomics and microbiome samples of the control group were not sequenced. Dietary restriction has metabolic benefits. A number of studies have reported that dietary restriction can affect the serum metabolites of healthy individuals, thus inducing anti-aging effects [24] and improving metabolic syndrome [25], etc. In this research, we focused on alteration in serum metabolomics before and after TRE.

The principal component analysis (PCA) plot illustrates a distinct separation between Day0 and Day30 samples, suggesting a significant change in the metabolic phenotype of volunteers induced by TRE (Fig. 4a). According to variable importance in projection (VIP) > 1 in orthogonal partial least squares discriminant analysis (OPLS-DA) model and $P < 0.05$ in T-Test, we screened 421 differential metabolites, with 219 up-regulated and 202 down-regulated in Day 30 than in Day 0 (Fig. 4b). And the heatmap illustrates 110 endogenous metabolites changes in metabolite abundance (Fig. 4c).

Furthermore, metabolite subclass analysis was performed to further explore their functional classifications (Fig. 4d). Enrichment analysis revealed that a significant portion of these differential metabolites are categorized under lipids (64.55 %) and proteins and amino acids (11.82 %) (Fig. 4d). Among lipids, glycerophospholipids (52.11 %), fatty Acids (18.31 %) and acyl groups (16.90 %) were the top three subgroups (Fig. 4e). The KEGG metabolic pathway analysis reveals that these differential metabolites were predominantly enriched in the glycerophospholipid metabolic pathway, cysteine and methionine metabolism and sphingolipid metabolism (Fig. 4f and g). Further, we analyzed the correlations between the $CD4^+CD27^-CD28^-$ cell frequency and differential metabolites (Fig. 4h). The results suggested that, the increased abundance of some anti-inflammatory lipids including N4-Acetylcytidine, PS(22:6(4Z,7Z,10Z,13Z,16Z,19Z)/22:2(13Z,16Z)), LysoPE(15:0/0:0), PC(16:2e/3:0) and LysoPC(22:4(7Z,10Z,13Z,16Z)) were negatively associated with a decrease $CD4^+CD27^-CD28^-$ cell frequency (Fig. 4i, Fig.S9). β-Tyrosine and 7a-Hydroxyandrost-4-ene-3,17-dione, of which the abundance reduced after 30-day TRE, were positively associated with a decrease in the frequency of $CD4^+CD27^-CD28^-$ cells (Fig. S8e, Fig.S9). In addition, we also observed significant correlations between differential metabolites and Treg cell frequency. The increased abundance of PA(16:0/18:2(9Z,12Z), PC(20:4(5Z,8Z,11Z,14Z)/14:0), PI(20:1(11Z)/18:2(9Z,12Z)) and sphingosine-1-phosphate (S1P) was negatively correlated with the increased frequency of Treg cell, whereas decreased abundance of Farnesylcysteine was positively correlated (Fig. S9).

TRE may alter the sphingolipid metabolism pathway, in turn plays anti-inflammatory and immune-enhancing effects. The results showed the serum level of S1P and L-serine, enriched in the sphingolipid metabolism pathway, were significantly increased (Fig. S8a). Subgroup analysis revealed lower baseline L-serine levels in the >30y group, which remained stable after TRE, while S1P levels showed no difference (Fig. S8b). Specifically, S1P, a potent bioactive lipid [26], could delay senescence [27] and enhance immune cell functions [28]. L-serine can not only suppress inflammation and oxidative stress by inhibiting the hypoxia-inducible factor α pathway [29], but also maintain neuronal development and brain function, restore cognitive function and inhibit inflammation [30]. Increased levels of S1P and L-serine suggest TRE may exhibit potential anti-aging and essential processes regulating effects (Fig. S8a).

After TRE, the serum level of 5′-Methylthioadenosine (5′-MTA) decreased and 2-ketobutyric acid (α-KB) increased both in total and the age subgroup (Fig. S8a and b). They are the meaningful differential metabolites in the cysteine and methionine metabolism pathway, which are characterized as anti-inflammatory factors. 5′-MTA inhibits TNF-α expression in macrophages and can alleviate inflammation-induced colon cancer [31]. While α-KB inhibits anti-inflammatory responses by altering glycine metabolism, reduction in α-KB was found to impair anti-inflammatory effects [32]. And supplementation with α-KB reduces mammalian cellular senescence and prolongs lifespan by promoting peroxisome function in *Cryptomeria hidradii nematodes* [33].

TRE can remodel lipid metabolism, in turn inhibiting inflammation and anti-aging effects. 30-day TRE increased the serum levels of PE (14:1/14:0), PC(22:6/22:5), LysoPC(15:0) and PA(16:0/18:2) (Fig. S8c), which were enriched in glycerophospholipid metabolism pathway. In the age subgroup analysis, PE(14:1/14:0) and PC(22:6/22:5) levels were significantly increased in the <30 y group and had a comparatively higher baseline in the >30 y group, whereas LysoPC (15:0) and PA(16:0/18:2) levels were elevated in serum from both age groups (Fig. S8d). Studies have revealed that the normal levels of phosphatidyl ethanolamine (PE) can decline with age in the brain, acting as a protective factor against aging-related diseases [34]. Particularly, introducing PE into *Caenorhabditis elegans* has been shown to enhance their anti-oxidative stress defense activity and effectively counteract the decline in muscle function due to aging. In addition, apoptotic cells release lysophosphatidylcholine (LysoPC) to recruit macrophages to clear themselves [35], which prevents inflammatory responses caused by cellular debris. PE and phosphatidylcholine (PC) have been found to prolong the organism's lifespan by downregulation of the insulin/IGF-1-like signaling pathway [36].

2.9. TRE shifted gut microbiota toward youthful composition by increasing alpha diversity and abundance of Akkermansia and Rikenellaceae

The gut microbiota shows varying characteristics with aging and is directly linked to the host's health and longevity. Studies have found that the intestinal microecological structure of aged individuals differs from that of young individuals [37], while centenarians and young people share a similar gut microbiota composition [38]. Therefore, we performed 16S DNA amplicon sequencing to investigate the effects of 16:8 TRE on the gut microbiota and how these effects relate to aging.

In microbiology, quantifying biodiversity is a vital aspect of research. In this study, we assessed the diversity of the gut microbiome before and after TRE by analyzing alpha diversity, beta diversity, Chao's index and Amplicon sequence variables (ASVS). Alpha diversity can show the richness of species in a community and the evenness of the number and distribution of each species. Beta diversity describes the species diversity between two communities or ecosystems. The Chao index estimates the total species richness of a community by calculating rare species. ASVS groups similar DNA sequences into one ASV via high-throughput sequencing, allowing for the analysis of microbial community diversity, composition, and structure. In this research, the Chao1 diversity index was higher on Day 30 than on Day 0 (Fig. 5a) with a more pronounced increase in the <30y group (Fig. S10a). However, there is no significant difference in Shannon index and beta diversity (Fig. 5b, Fig. S10 a&f). The ASVS for the gut microbiota was higher on Day 30 (Fig. 5c) with a more pronounced increase in the >30y group (Fig. S10c). These results suggest a significant elevation in microbiome alpha diversity.

At the phylum level, after a 30-day TRE, the relative abundances of *Firmicutes* and *Proteobacteria* decreased, while those of *Bacteroidetes* and *Actinobacteria* showed an increasing trend (Fig. 5d). Age subgroup analyses showed that these changes were more pronounced in the >30 year group (Fig. S10b). The gut microbiome seems to be more significantly impacted by TRE in >30y individuals.

At the genus level, our study observed a notable increase in the relative abundances of the genera *Akkermansia* and *Rikenellaceae* (Fig. 5e). While we found no statistical significance in age subgroup

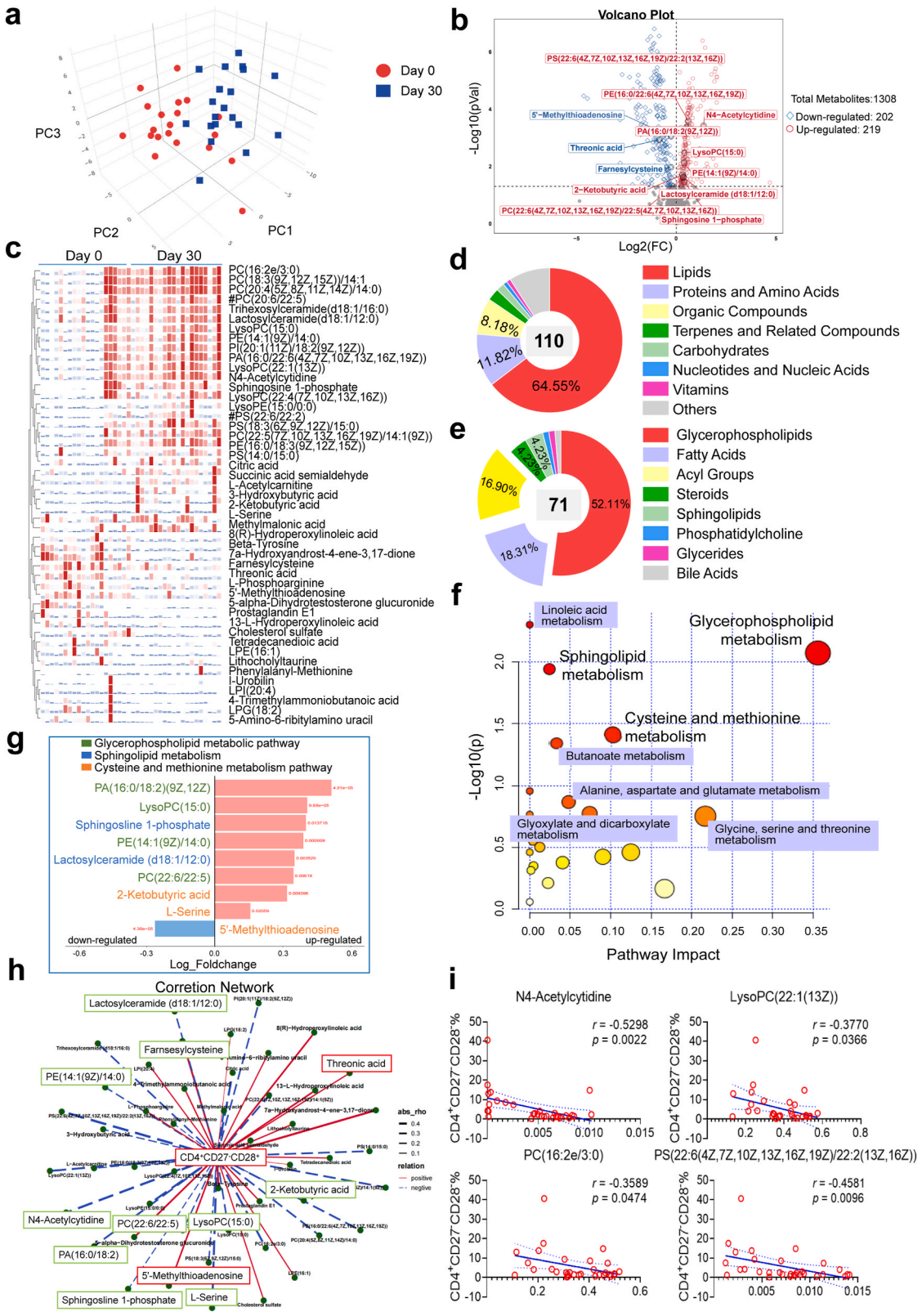

Fig. 4. Metabolic differences before and after 30-day TRE. (a) Score scatter plot of the OPLS-DA model for metabolites on Day 0 and Day 30 of TRE; (b) Volcano plot of differential metabolites on Day 0 and Day 30 (VIP >1 and $P < 0.05$ in paired *t*-test); (c) Heatmap showing the metabolite abundances in participants before and after TRE. The 110 differential metabolites (d) and 71 subclasses of lipid and lipid-like molecules (e) after TRE. (f) KEGG metabolic pathway analysis in participants before and after TRE; (g) Analysis of pathway-based differential metabolites after TRE; (h) and (i): correlation analysis between $CD4^+CD27^-CD28^-$ cell frequency and metabolite abundances; Abbreviations: #PC(20:6/22:5): PC(20:6(4Z,7Z,10Z,13Z,16Z,19Z)/22:5(4Z,7Z,10Z,13Z,16Z)); #PS(22:6/22:2): PS(22:6(4Z,7Z,10Z,13Z,16Z,19Z)/22:2(13Z,16Z)); TRE Day 0 group, n = 20; TRE Day 30 group, n = 20, these two groups used the same subject's samples before and after TRE. Statistical analysis was performed using Spearman's correlation coefficients in Fig. 4i.

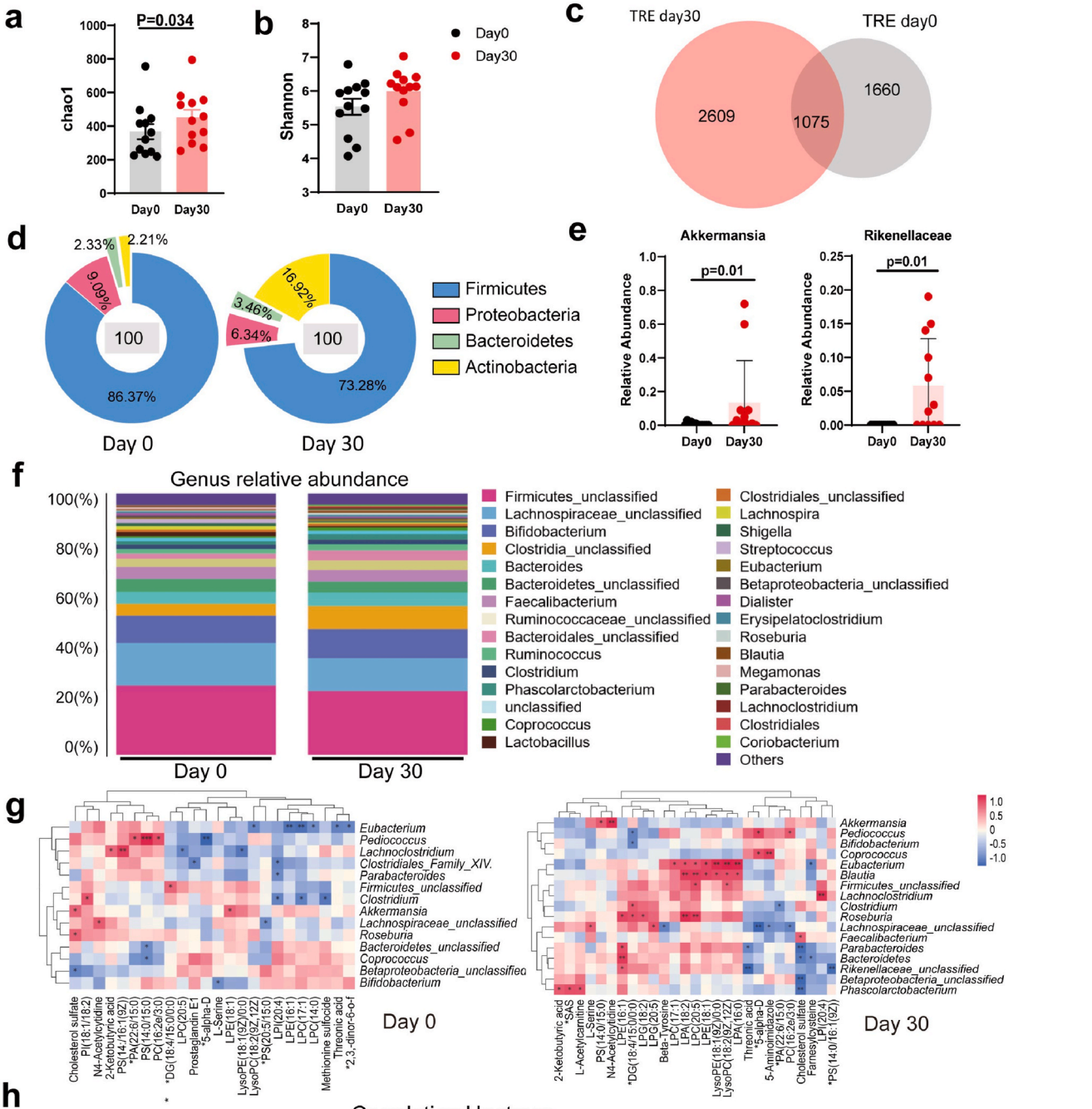

(caption on next page)

Fig. 5. Gut microbiome differences before and after 30-day TRE. (a) The Chao1 community richness index, (b) Shannon index and (c) the total number of amplicon sequence variants (ASVs) observed before and after TRE; (d) Changes in the phylum distribution of gut microbiomes before and after TRE; (e) Changes in abundance of *Akkermansia* and *Rikenellaceae* before and after TRE; (f) Changes in the genus distribution of gut microbiomes before and after TRE, only the top 30 predominant taxa are shown. (g) Correlation analysis between genus and differential metabolites on Day 0 and Day 30. (h) Correlation analysis between genus and the frequencies of Sene, Th1, Th2, Th17 and Treg cells. TRE Day 0 group, n = 12; TRE Day 30 group, n = 12. Abbreviations: *un: unclassified; Clostridiales_Family_XIV: *Clostridiales_Family_XIV._Incertae_Sedis_unclassified. Statistical analysis was performed using the paired Wilcoxon test at two different time points, as shown in Fig. 5a, and the paired *t*-test was performed in Fig. 5a,b&e. Data are the mean ± s.e.m.

analysis (Fig. S10d). Additionally, we detected changes in the relative abundances of several other flora after TRE, as shown in Fig. 5f and Fig. S10e. These included an increase in certain butyric acid-producing bacteria, such as *Clostridiales_ unclassified*, *Eubacterium*, *Coprococcus*, and *Clostridiales*, as well as other genera like *Blautia*, *Phascolarctobacterium*, *Bifidobacterium*, and *Roseburia*. On the basis of increased α-diversity and a rise in the number of beneficial bacteria, we also observed that the microbial community structure of the two age groups became more consistent after TRE (Fig. S10e). However, these variations did not reach statistical significance. In general, while only the alterations in *Akkermansia* and *Rikenellaceae* were statistically significant, the overall trend in the gut microbiome composition indicated a shift toward patterns observed in centenarians and young adults.

To identify all genera that were associated with serum metabolites, we investigated the associations of genus-level abundances (Fig. 5g, Fig. S11) with serum metabolites, and Spearman's correlation coefficients were applied. We observed a shift in the association of microbial species with metabolites from Day0 to Day30 of TRE, suggesting that TRE may influence the dynamic interactions between gut microbes and serum metabolites (Fig. 5g). Specifically, we found that the serum level of N4-acetylcytidine, PC (16:2e/3:0) and phosphatidylserine (PS) (14:0/15:0) were positively correlated with *Akkermansia*. N4-Acetylcytidine, a conservative chemical modification in eukaryotic prokaryotes, is negatively related to inflammation [39]. Threonic acid and cholesterol sulfate, which are positively associated with metabolic diseases and stress, were negatively correlated with *Rikenellaceae* [40]. The results showed that TRE affects material metabolism in part through the gut microbiota. Further, we also analyzed the correlation between gut microbial species and immune cell subsets (Fig. 5h). Decreased abundance of disease-associated *Burkholderia* and *Thiohalomonas* was positively correlated with a decrease in senescent T-cells, whereas decreased abundance of *Burkholderia* was also positively correlated with a decrease in Th2 cells. Increased abundance of *Clostridiales_unclassified* was negatively correlated with decreased frequencies of Th2 and Th17 cells, while increased abundance of *Eubacterium* was negatively correlated with decreased frequency of Th17 cells. Increased abundance of *Phascolarctobacterium* was negatively correlated with increased Th1 cell frequency. Together, these results highlight the potential role of gut microbes in modulating host immune responses (Fig. 5h).

3. Discussion

TRE is commonly used to fight obesity. It could be an effective, economical, safe and simple form of treatment for reducing weight, improving metabolism, and even fighting aging. The senescence of immune cells is the core factor of body senescence, and serum metabolomics and intestinal microbiota are associated with the status of immune cells. Therefore, we provided the concept that TRE is not just for weight loss but can achieve anti-aging effects and improve metabolism by "refreshing" the immune system and intestinal microecology.

After the 30-dayTRE, a decrease in BMI within the normal range was observed. Meanwhile, parameters including body fat rate, visceral fat, and fat weight decreased, while body moisture and skeletal muscle rate increased. Body moisture usually refers to the water inside the body, but it also decreases with age and decreases with obesity. Also, most participants expressed that they get reduced physical burden, gastrointestinal comfort, good mental outlook and happy mood during the TRE. These data were subjective feelings from the questionnaire and were hard for statistical analysis. To sum up, TRE is a relatively healthy way to lose weight.

However, muscle mass and basal metabolic rate decreased after TRE, but dieting inherently causes muscle loss and reduces lean muscle tissue, further reducing basal metabolism, which is consistent with our observations. Exercise prevents lean muscle tissue loss and increases the amount of lean muscle tissue, which is the most effective way to promote basal metabolic rate [41]. Thus, TRE combined with proper exercise and calorie intake adjustment may be an even better way to lose weight.

We evaluated the effect of TRE on immune system function in terms of (1) the frequency of immune cell subsets in PBMCs and (2) the composition of the IR in PBMCs before and after 30 days of TRE.

After 30-day TRE, the differences were mainly manifested in $CD4^+$ T-cell subsets. Previous studies also showed that $CD4^+$ T cells mediated obesity memory and promoted weight regain after weight loss [42]. Obesity and metabolic syndrome have potential connections with immune diseases [43,44]. In detail, our results showed that the frequency of Th2 and Th17 cells decreased. Additionally, the frequencies of Treg and Tfh-like cells increased after TRE. Increased frequency of circulating Tfh-like cells was observed, suggesting higher humoral immune responses after TRE. However, when we detected the Ig levels after TRE, there was no significant difference. Circulating Tfh-like cells in humans might not really reflect the germinal center responses and Ig production.

Senescent cells are key drivers of aging, and their elimination can alleviate many age-related diseases [45]. In the process of aging, many cells will exhibit senescence phenotypes, but immune cell senescence is the most harmful. Studies have shown that immune cell senescence can exacerbate the whole body's aging [46]. Our findings suggest that 30-day TRE treatment can reduce $CD4^+$ senescent T cells and may serve as an anti-$CD4^+$ T-cell senescence therapy. According to Li et al., the 30s and 50s are transitional periods during Chinese women's aging [17]. Therefore, we further stratified the analysis of data from subjects >30y and <30y. We were pleasantly surprised to see that the decrease in >30y became more pronounced.

Regarding the IR, the normal body constantly encounters a variety of antigens, both endogenous and exogenous. The detection of monoclonal rearrangement of the BCR gene indicates pathological status, such as infection [47] and autoimmune diseases [48]. The significantly reduced large clones of heavy, kappa and lambda BCR chains (Fig. 3b) showed that TRE was able to improve immune system function in healthy individuals. Despite changes in the proportion of immune cell subsets, there was no difference in IR diversity between TRE and its predecessors (Figs. S6b and c). The higher the IR diversity is, the more robust the immune system. Thus, the 30-day TRE was able to eliminate immune-senescent cells without affecting the functions of immune cells. However, TRE decreased all CSR index values, indicating that B-cell activation ability was reduced and that TRE therapy may impair humoral immune responses, which still needs to be confirmed by further experiments.

Changes in serum metabolites showed a clear anti-inflammatory effect after 30-day TRE, which is consistent with previous studies [49,50]. In short, the abundance of some metabolites with anti-inflammatory effects (PE, PC, LysoPC, S1P, α-KB, L-serine and N4-Acetylcytidine) increased. Notably, the shifts in these metabolite levels are strongly linked to the reduction of senescent T cells and the rise in Treg cells, indicating that TRE might enhance health by regulating immune responses. Among them, S1P is an important bioactive lipid, in inflammatory or infectious situations, its concentration gradient plays a key

role in the migration of T cells from the lymph nodes (relatively lower concentration) to the tissues and eventually into the blood (relatively higher concentration) [51]. In addition, the duration of T cells in the lymph node is thought to be an important factor in regulating their differentiation [52]. It has been shown that a decrease in S1P concentration contributes to the maintenance of the central memory T cell and hinders the differentiation of Naïve T cells to Treg by inhibiting the PPARγ pathway [53]. After 30-day TRE, an observed increase in Treg cell frequency and a corresponding decrease in Th17 and Th2 cells in PBMCs may suggest a regulatory influence of S1P on T cell differentiation. Although a negative correlation was found between S1P levels and Treg cell frequency, the precise regulatory mechanisms of S1P on T cell differentiation require further study. These findings provide new perspectives for understanding the role of S1P in immune regulation. Additionally, other anti-inflammatory metabolites, which showed a similar negative correlation with Treg cell frequency, merit further investigation into their relationship with T cell regulation.

Enrichment analysis of differential metabolites identified two potential pathways after TRE intervention: glycerophospholipid metabolic pathway and cysteine and methionine metabolism pathway. A study in RA patients revealed a significant negative correlation between glycerophospholipids and inflammatory markers like erythrocyte sedimentation rate (ESR), C-reactive protein (CRP), and IL-6, as well as age, and also a negative correlation with leukocyte counts. This indicates a potential anti-inflammatory role of the glycerophospholipid pathway [54]. Cysteine and methionine are important amino acids, and their metabolic pathways are important for the body's antioxidant and free radical elimination functions. The cysteine methionine pathway has been found to help enhance resistance to stressful environments [55]. The enrichment of differential metabolites in this pathway suggests that TRE may augment the body's antioxidant defenses to a certain degree.

As for gut microbiota, it tightly links to the health and longevity. On the one hand, high microbial diversity supports gut ecosystem stability and resilience, with a healthy microbiome marked by abundant Bacteroidetes and Firmicutes, high levels of probiotics like *Bifidobacterium*, and the production of short-chain fatty acids (SCFAs) like acetic and butyric acid [56]. On the other hand, the composition of microbiota changes with age, stabilizing by age 3–5 and varying due to lifestyle, diet and so on, with major changes in old age (>65). Notably, the microbiota of healthy elderly or centenarians resembles that of the 30s [57–59].

We also found some meaningful results regarding the gut microbiota in this research. After 30-TRE, a significant increase in the alpha diversity of gut microbes was observed, along with an increase in the abundance of key microbial populations such as *Akkermansia* and *Rikenellaceae*. *Akkermansia,* a beneficial gut probiotic, has been shown to prevent obesity, improve glucose tolerance, extend lifespan [60] and possess anti-inflammatory properties [61]. Interestingly, although its relative abundance decreased with age, it was comparable to that of young adults in centenarians [37]. The genus *Rikenellaceae* spp. is more abundant in lean individuals and is considered a potential indicator of healthy aging and longevity [62].

In addition, the relative abundance of some butyrate-producing bacteria increased with no significant statistical differences (*Clostridiales_unclassified, Roseburia, Clostridiales, Parabacteroide, Blautia and Eubacterium*).These bacterial genera, which tend to decrease in abundance in the elderly, show similar levels in centenarians and young individuals [57,63,64], and possess anti-inflammatory [65] and anti-obesity potential [66]. Studies also indicate that an increase in butyrate-producing bacteria is associated with reduced frailty and inflammation, as well as improved cognitive function [67]. Moreover, the relative abundance of β-proteobacteria, which decreases in centenarians [39], also declined after TRE. These results suggest a trend towards a "younger" and "healthier" composition of the gut microbiota.

In the correlation analysis, we found that serum metabolomics and gut microecology of healthy participants showed significant anti-inflammatory trends through a 30-day TRE intervention. Specifically, metabolites negatively associated with inflammation, such as N4-acetylcytidine, showed a positive correlation with *Akkermansia* abundance [39]. Meanwhile, metabolites positively associated with metabolic diseases and stress, such as threonine and cholesterol, showed a negative correlation with Rikenellaceae abundance [40,68]. The association analysis results marked an anti-inflammatory trend in serum metabolomics and intestinal microecology in healthy participants after a 30-day TRE intervention. Moreover, three genera, *Clostridiales_unclassified*, *Eubacterium* and *Phascolarctobacterium*, produce SCFAs in the gut. Their increased abundance is negatively correlated with changes in Th cell subsets. SCFAs promote the release of the anti-inflammatory cytokine IL-10, inhibit pro-inflammatory factors, and maintain intestinal immune homeostasis through the activation of G protein-coupled receptors (GPR) such as GPR43 and GPR41 [69,70]. In addition, SCFAs play an anti-inflammatory role by regulating T cell differentiation [71,72], which is consistent with the negative correlation we observed. These results suggest that TRE remodels the intestinal microecology and helps reduce intestinal inflammation.

Undoubtedly, this study is subject to the limitations inherent in clinical trial design. Due to these constraints, our capacity to enroll a sufficiently large cohort of age-matched control subjects was compromised, and it was not viable to subject the control group samples to a comprehensive panel of biomarker assessments. Consequently, individuals around the age of 50 were less willing to participate in our TRE clinical trial, which posed a considerable challenge in volunteer recruitment. Next, the analytical strategy employed in this study predominantly relied on comparisons of the participants' biomarker profiles before and after TRE. Furthermore, there was a significant loss of follow-up among subjects in the extended post-intervention period, which may impact the robustness of our long-term findings. Similarly, in aging-related studies, subjects may not be old enough to effectively assess the effects of TRE on aging. Despite these challenges, our findings indicate a pronounced improvement in immune senescence metrics among female participants over the age of 30, suggesting a heightened susceptibility of older individuals to the beneficial effects of TRE.

The multi-omics and correlation analyses have revealed the mutual connections between the frequency of immune senescent cells, serum metabolites, and the gut microbiome. (Fig. 4h–i, Fig. 5h). Overall, the reduction in the frequency of immune senescent cells is the most compelling evidence of the effectiveness of TRE intervention. Concurrently, we observed an upregulation of beneficial metabolites (such as PE, PC, LysoPC, S1P, α-KB, L-serine, and N4-acetylcytidine) and an increase in the abundance of microbiota associated with longevity (such as *Akkermansia* and *Rikenellaceae*). These data suggest a comprehensive shift towards a "younger" state post-TRE.

In conclusion, all the evidence suggests that TRE, as a dietary intervention, is not just beneficial for weight loss but also reveals a "younger" immune system and intestinal microbiome.

4. Methods

4.1. Study registration

The study was carried out with the agreement of the Second Xiangya Hospital's ethical committee and in compliance with good clinical practice and the International Declaration of Helsinki (GCP). The clinical examinations were conducted at the Hunan Key Laboratory of Medical Epigenomics at the Second Xiangya Hospital, China. The study was registered at chictr.org.cn (ChiCTR2200058137).

4.2. Participants

We recruited a total of 59 participants from the area around the Second Xiangya Hospital (<3 km), Hunan Province, through posters and social media and they were all available to participate in the clinical trial in the laboratory. 49 participants formed the TRE group and 10

participants formed the control group. The trial recruited participants who consumed food over 8 h per day and had not fasted in the last year. All participants should meet the inclusion criteria and not the exclusion criteria. The consort diagram can be found in Fig. S1, and baseline information for each group is presented in Table 1.

This study focused on dietary timing adjustments and used a single-arm design without implementing blinding or randomization procedures Participants who met the criteria and volunteered to participate in TRE were included in the study. Volunteers who lived in the same area and had similar living habits as TRE volunteers were included in the control group, which was mainly used to reduce errors in the analysis of IR.

4.3. Outcomes

The primary and secondary outcome measures are as follows [Time window: 30 days (from baseline to 30 days)]: (A) Primary outcome metric: $CD4^+CD27^-CD28^-$ senescent T cell frequencies in PBMCs. Flow cytometry was used to detect changes in the frequencies of senescent T cells in PBMCs. (B) Secondary outcome indicators: (1) weight changes and other weight-related index: body moisture, skeletal muscle, body fat rate, BMI, muscle mass, visceral fat, bone mass, basal metabolism and fat weight. (2) Frequencies of each immunocyte and immunosenescent cell in PBMC. Flow cytometry detection of changes in the frequencies of the following immunocytes: (a) each subset of T cells ($CD4^+$ T cells, $CD4^+$ Naive T cells, $CD4^+$ Effector T cells, Th1, Th2, Th17, Treg, Tfh-like, $CD8^+$ T cells, $CD8^+$ Naive T cells, $CD8^+$ Memory T cells). (b) B cell subpopulation (total $CD19^+$ B cells, Naive B cells, Memory B cells, and plasma cells). (c) $CD27^-CD28^-$ immunosenescent cells in each subset. (3) Serum metabolomics: LC-MS metabolomic analysis was applied to detect changes in serum metabolites. (4) Immune repertoire (IR): IR refers to the sum of all functionally versatility T cells and B cells in the circulatory system of individuals. (5) Gut microorganism: 16S rDNA sequencing analysis was applied to detect changes in intestinal microecology.

4.4. Inclusion criteria and exclusion criteria

The inclusion criteria were as follows: (1) 18–60 years old, both inclusive; (2) weight stability (change $< \pm 10$ % from current body weight) for Day90 before trial (3) BMI over 18.0 kg/m^2, both inclusive; (4) no cardiovascular or metabolic diseases; (5) no acute or chronic inflammation; (6) no drugs; (7) no alcohol abuse; (8) no dietary restrictions (e.g., vegetarian); (9) no; gastrointestinal diseases. The exclusion criteria were as follows: (1) eating disorder history; (2) malignancy confirmed by biopsy; (3) pregnancy, breastfeeding or trying to conceive; (4) hormone supplements or anti-fertility hormone drugs (for over 2 months); (5) received antidepressant medication within the past 6 months; (6) intake of nonsteroidal anti-inflammatory drugs (NSAIDs).

Table 1
Characteristics of baseline.

Characteristic	TRE (Total)	TRE (<30 y)	TRE (>30y)	Control
No.	49	20	29	10
Age, mean (SD), years	33.2 (8.50)	25.5 (2.11)	38.5 (6.85)	25.1 (1.60)
Female	44 (89.8 %)	18 (90.0 %)	26 (89.7 %)	7 (70 %)
Weight, mean (SD), kg	63.2 (10.1)	61.6 (6.3)	64.3 (11.8)	56.55 (11.9)
BMI, mean (SD)	24.0 (3.9)	22.7 (2.4)	24.9 (4.3)	20.84 (2.6)

BMI: body mass index (BMI = kg/m^2), TRE: time-restricted eating, Data are mean (SD).

Table 2
Identify maker of cell subsets for flow cytometry.

Cell subset	Identify marker
$CD3^+$ T	$CD3^+$
$CD4^+$ T	$CD4^+$
$CD8^+$ T	$CD8^+$
$CD4^+$ naïve T	$CD45RO^-CD45RA^+CD4^+$
$CD4^+$ effector T	$CD45RO^+CD45RA^-CD4^+$
Th1	$CXCR3^+CCR6^-CCR4^-CD4^+$
Th2	$CXCR3^-CCR6^-CCR4^+CD4^+$
Th17	$CXCR3^-CCR6^+CCR4^+CD4^+$
Tfh-like	$CXCR5^+PD\text{-}1^+CD4^+$
Treg	$CD127^{lo}CD25^{hi}CD4^+$
$CD45RA^+CD8^+$ T	$CD45RA^+CD8^+$
$CD45RA^-CD8^+$ T	$CD45RA^-CD8^+$
Senescent $CD4^+$ T	$CD27^-CD28^-CD4^+$
Total $CD19^+$ B	$CD19^+$
Memory B	$CD38^-IgD^-CD27^+CD19^+$
Naive B	$CD38^-IgD^+IgM^+CD19^+$
Plasma cell	$CD38^+CD20^-CD19^+$

4.5. Grouping dietary interventions and intervention supervision

The TRE group ate during the daily period from 9 a.m. to 5 p.m. with a 24-h cycle. Participants in the TRE group were provided nutritious meals by the nutrition canteen of the Second Xiangya Hospital from 9 a.m. to 10 a.m., 12 a.m.-1 pm, and 4 p.m.–5 pm every day for 30 days. The recipes were carefully designed by clinical nutritionists based on *The Chinese Dietary Guidelines (2016 edition)* to ensure a balanced nutritional profile. The daily diet is shown in Table S1. The clinical nutritionist calculated each volunteer's basal metabolic rate by referring to the Mifflin-St. Jeor equation [73] and then multiplied it by the daily exercise (an appropriate factor), resulting in a nutritious meal with slightly more calories than the daily energy requirement per meal (A. infrequent exercise, a lot of sitting work: 1.1; B. moderate exercise, a lot of sitting work: 1.3; C. frequent exercise, a lot of physically active work: 1.5; D. a lot of exercise, a lot of physically active work: 1.7). Participants in the control group did not undergo any specific interventions since their daily diets are quite similar to nutritious meals provided by nutrition canteen. As a result, the daily calories and nutrients consumed by the two groups were roughly similar, except for the inconsistent eating times.

Participants were expected to take pictures of their meal while eating it as well as after they completed it and to submit them to the investigators using WeChat as part of the compliance criteria. If the TRE participants failed to post a meal photo, they were reminded in an hour. It was considered a failure to complete the trial if participants missed uploading those photos nine times (or three days). The uploaded photos were checked daily to ensure that participants consumed enough nutrition.

4.6. Samples collection

4.6.1. Human peripheral blood sample collection

A sterile vacuum blood collection tube was used for each group to collect 15 ml of fresh EDTA-anticoagulated peripheral venous blood and 3 ml of procoagulant at Day 0, Day 14, and Day 30. We also took blood samples from participants on Day 90 after TRE to understand the long-term effects. Table 1 presents the detailed baseline characteristics of the TRE participants.

4.6.2. Stool sample collection

We collected stool samples from each subject on Day 0 and Day 30, transferred them into liquid nitrogen for quick freezing for 2 min within 1 h, and preserved them at −80 °C to send for 16S rDNA microbiome sequencing.

4.7. Body weight and weight-related indicators analysis

The weight and weight-related indicators of all participants were measured using the same multifunctional body mass measuring instrument. The instrument uses an electrical resistance method to measure body fat percentage and body moisture. The instrument can measure indicators including body weight, body fat rate, BMI, muscle mass, body moisture, visceral fat, bone mass, basal metabolism, fat weight and skeletal muscle rate. On Day 0, Day 7, Day 14, Day 21 and Day 30 of this trial, the body weight and other weight-related indicators of the participants in their fasting were measured at 8 a.m. Notably, in order to rule out post-eating disturbances, the participants were also asked not to eat breakfast and drink too much water at baseline weight measurements.

4.8. Flow cytometry analysis

PBMCs were separated from fresh EDTA-anticoagulated peripheral venous blood using Ficoll-Paque™ PLUS (cytiva, 17144003). Approximately two million cells per tube suspended in phosphate-buffered saline (PBS) were mixed with labeled surface antibodies for 45 min in the dark at 4 °C to fully bind. FlowJo software (V10.5.3) was used to analyze flow cytometry data. All flow cytometry data were acquired by a DxP Athena™ flow cytometer (Cytek, US). The flow cytometry antibodies and kits used are listed in the Supplementary Table S2.

4.9. Immune repertoire analysis

The PBMC samples of the top five subjects with the largest reduction in the proportion of immunosenescent cells in the >30 y group and the <30 y group were selected for sequencing, and five control samples were tested at the same time. IR analysis was supported by Nanjing ARP Biotechnology Co., Ltd., and the extracted total RNA was amplified using the commercially available iR-RepSeq-plus 7-Chain Cassette (iRepertoire Inc., US) covering all 7 chains of the human TCR and BCR through a reverse transcription technique that incorporates unique molecular identifiers. Using one disposable cassette with preloaded reagents for amplification and purification, human TCR and BCR libraries were constructed, and RT was performed using OneStep RT−PCR mix (Qiagen). Amplification of the library was accomplished using primers engineered specifically for communal site primers. SPRIselect bead selection (Beckman Coulter) was used to remove unused primers from first-strand cDNA. V-gene primer mix was then used for the second binding and extension round. Using a 600-cycle kit, amplified libraries were multiplexed, pooled, and sequenced on the Illumina MiSeq platform. The iRmap tool was used to analyze the raw sequencing data [74]. Details of this IR methodology have been described previously [75]. Sequence analysis was finished in GitHub, and the data were exported to Microsoft Excel (Microsoft 365).

4.10. LC-MS metabolomic analysis

Serum samples were selected from the top 20 participants in the TRE group, who displayed a decreased proportion of immunosenescent cells, for untargeted metabolomics analysis. Samples were obtained on Day 0 and Day 30, all during their fasting state at around 8 a.m. Metabolomics analysis was accomplished in the laboratory or with the assistance of Shanghai Biotree Biotech Co., Ltd. A total of 12,241 peaks were extracted from the original data package, and a single peak of the original data was filtered to remove noise, filtered and filled with missing values, and normalized with an internal standard (IS), in which Student's *t*-test was applied. For the multivariate statistical analysis, SIMCA software (V16.0.2) was used [76,77]. The data were analyzed by PCA. OPLS-DA of the metabolites removed orthogonal variables not relating to categorical variables. To obtain more reliable information on metabolite group differences and their relevance to the experiments, we analyzed the orthogonal variables separately from the nonorthogonal variables. We first analyzed the OPLS-DA model on the first principal component based on logarithmically transformed and UV-formatted data. The quality of the model was checked using sevenfold cross-validation. The validity of the model was then assessed using the cross-validation results. A permutation test was used to further examine the validity of the model. An additional assessment of the robustness was performed on the OPLS-DA model with a permutation test. Using the combined findings of statistical analysis of unit variables and multivariate variables, the differential metabolites were filtered out following the aforementioned analysis. The chi-square value of multivariate statistical analysis has the following two criteria.

1. The p-value of Student's *t*-test was less than 0.05; 2. The VIP value is greater than 1. Hierarchical clustering was used to analyze the results of the screened differential metabolites and the functional similarity/complementarity features.

We identified metabolites by searching the KEGG database and HMDB database (https://hmdb.ca/). Pathway enrichment analysis was performed using MetaboAnalyst 5.0[78].

4.11. 16S rDNA microbiome sequencing

16S DNA amplicon sequencing was performed on fecal samples from 12 healthy participants. Microbiome sequencing analysis was accomplished with assistance from Shanghai Biotree Biotech Co., Ltd. On Day 0 and Day 30 of the study, stool samples were collected from the relevant groups. The total DNA of the stool microbiome was extracted with the E.Z.N.A.®Stool DNA Kit [79]. The hypervariable V3–V4 region of bacterial 16S rDNA was sequenced on the NovaSeq PE250 platform [80,81], in which the primers 805R and 341F (5′-GACTACHVGGGTATCTAATCC-3′ and 5′-CCTACGGGNGGCWGCAG-3′, respectively) were applied. The manufacturer's instructions were followed for sequencing samples on the Illumina NovaSeq platform. Sample-specific barcodes were used to assign paired-end sequences to each sample, and primer sequences and barcodes added during library creation were removed. Matching end readings were combined using FLASH. Fqtrim (v0.94) claims that to produce high-quality clean labels, the raw read data were quality-filtered under particular filtering circumstances. Vsearch software was used to screen out chimeric sequences (v2.3.4) [82]. The feature table and feature sequence were retrieved using DADA2. By normalizing to the same random sequence, diversity was computed. Each sample's relative abundance was used to normalize feature abundance, which was determined by the SILVA classifier. Chao1 and alpha diversity were used to detect the species diversity of the samples. BLAST was employed for sequence alignment, and then we annotated unique sequences from the SILVA database on each representative sequence. We also computed Spearman correlations between the relative abundances of genera and serum metabonomics. The graphs were produced with Prism 8 and R (v3.5.2).

4.12. Statistical analysis

IBM SPSS® software and GraphPad Prism v.8.0.2 performed statistical calculations. For the data of the proportion of immune cell subsets in TRE group participants, if Mauchly's test of sphericity sig >0.5, tests of within-subjects effects were used for data analysis. If Mauchly's test of sphericity sig <0.5, the Greenhouse-Geisser was used for data analysis. In addition, the proportions of immune cell subsets at different time points were compared by paired *t*-test. For the IR sequence data, two-way ANOVA was used for statistical analysis. For statistical analysis of data before and after the trial, such as metabolomic analysis and microbiome sequencing, a two-tailed paired *t*-test and paired Wilcoxon test were used for statistical analysis. Data are presented as the mean ± s.e.m. ns = not significant. The sample size calculation was done for the

primary outcome only. The methodological principles of the statistical analyses for the age subgroups of the supplementary are the same as above. Sellami Maha et al. studied the changes in the number of immune cell subsets in human PBMCs after 12 weeks of intermittent fasting [83]. In Sellami Maha's study, the mean ± standard deviation of $CD4^+$ T cells in the experimental group and the control group were 1206.4 ± 225.41 mm^3 and 985.6 ± 216.14 mm^3. The α value was 0.05, the proportion of lost follow-up was 0.1, and the confidence was 0.95. Comparing the two independent sample means to estimate the sample size of the experimental group and the control group, the calculation results showed that 17 participants were required for the TRE group. Sample size calculations were performed using the MedSci Sample Size tools (MSST). All the statistical analyses were reviewed by Professor Irene Xy Wu, a statistical expert at Xiangya School of Public Health, Central South University, China.

CRediT authorship contribution statement

Yiran Chen: Writing – review & editing, Writing – original draft, Visualization, Project administration, Methodology, Investigation, Formal analysis. **Xi Li:** Writing – review & editing, Writing – original draft, Visualization, Project administration, Investigation, Formal analysis. **Ming Yang:** Methodology, Funding acquisition, Formal analysis. **Chen Jia:** Investigation, Formal analysis. **Zhenghao He:** Visualization, Formal analysis. **Suqing Zhou:** Visualization. **Pinglang Ruan:** Visualization, Data curation. **Yikun Wang:** Data curation. **Congli Tang:** Formal analysis. **Wenjing Pan:** Formal analysis. **Hai Long:** Methodology, Funding acquisition. **Ming Zhao:** Methodology. **Liwei Lu:** Formal analysis. **Weijun Peng:** Formal analysis. **Arne Akbar:** Formal analysis. **Irene XY. Wu:** Data curation. **Song Li:** Formal analysis. **Haijing Wu:** Writing – review & editing, Writing – original draft, Validation, Supervision, Project administration, Methodology, Funding acquisition, Conceptualization. **Qianjin Lu:** Writing – review & editing, Supervision, Methodology, Funding acquisition.

Data and code availability

In accordance with the participant's privacy agreement, personally identifying information is not released in this article but may be shared by the corresponding author in special circumstances.

The paper does not report the original code. Any additional information required to reanalyze the data reported in this paper is available from the lead contact upon request.

Declaration of generative AI in scientific writing

The authors declare that the ChatGPT 4.0 was used to improve readability and language of this manuscript. The authors remain fully responsible and accountable for the content of the work.

Funding

This work is supported by the National Key R&D Program of China, No. 2022YFC3601800 (Q. Lu), funding from the Ministry of Science and Technology of the People's Republic of China, China. The Special Program of National Natural Science Foundation of China, No. 32141004 (Q. Lu), funding from the National Natural Science Foundation of China (NSFC), China. CAMS Innovation Fund for Medical Sciences (CIFMS) No. 2021-I2M-1–059 (Q. Lu), Non-profit Central Research Institute Fund of Chinese Academy of Medical Sciences No. 2021-RC320-001 (Q. Lu), National Natural Science Foundation of China (NSFC) No. 82173425 (H. Wu), No. 82373488 (H. Wu), No. 82273540 (H. Long), No. 82473530 (M. Yang), Natural Science Foundation of Hunan Province of China No. 2024JJ4077 (M. Yang).

Declaration of competing interest

The authors declare that they have no known competing financial interests or personal relationships that could have appeared to influence the work reported in this paper.

Acknowledgements

We would like to thank Dr. Zhidan Zhao, Dr. Di Long, and Dr. Suqing Zhou for their guidance on the experimental procedures. We thank the nurses and technicians of the Second Xiangya Hospital for their assistance in sample collection and assistance in volunteer reception. The study was carried out with the agreement of the Second Xiangya Hospital's ethics committee and in compliance with good clinical practice and the International Declaration of Helsinki (GCP). The clinical examinations were conducted at the Hunan Key Laboratory of Medical Epigenomics at the Second Xiangya Hospital, China. The study was registered at chictr.org.cn (ChiCTR2200058137). All participants volunteered to participate in the study and provided written informed consent. All data needed to evaluate the conclusions in the paper are present in the paper and/or the Supplementary Information.

Appendix A. Supplementary data

Supplementary data to this article can be found online at https://doi.org/10.1016/j.redox.2024.103422.

Data availability

No data was used for the research described in the article.

References

[1] M. Blüher, Obesity: global epidemiology and pathogenesis, Nat. Rev. Endocrinol. 15 (2019) 288–298, https://doi.org/10.1038/s41574-019-0176-8.
[2] A.J. Cox, N.P. West, A.W. Cripps, Obesity, inflammation, and the gut microbiota, Lancet Diabetes Endocrinol. 3 (2015) 207–215, https://doi.org/10.1016/S2213-8587(14)70134-2.
[3] W. Ying, et al., Expansion of islet-resident macrophages leads to inflammation affecting β cell proliferation and function in obesity, Cell Metabol. 29 (2019), https://doi.org/10.1016/j.cmet.2018.12.003.
[4] K. Shirakawa, et al., Negative legacy of obesity, PLoS One 12 (2017) e0186303, https://doi.org/10.1371/journal.pone.0186303.
[5] F. Cignarella, et al., Intermittent fasting confers protection in CNS autoimmunity by altering the gut microbiota, Cell Metabol. 27 (2018), https://doi.org/10.1016/j.cmet.2018.05.006.
[6] H. Müller, F.W. de Toledo, K.L. Resch, Fasting followed by vegetarian diet in patients with rheumatoid arthritis: a systematic review, Scand. J. Rheumatol. 30 (2001).
[7] V.D. Longo, S. Panda, Fasting, circadian rhythms, and time-restricted feeding in healthy lifespan, Cell Metabol. 23 (2016) 1048–1059, https://doi.org/10.1016/j.cmet.2016.06.001.
[8] Z. Xie, et al., Randomized controlled trial for time-restricted eating in healthy volunteers without obesity, Nat. Commun. 13 (2022) 1003, https://doi.org/10.1038/s41467-022-28662-5.
[9] S. Byun, et al., Fasting-induced FGF21 signaling activates hepatic autophagy and lipid degradation via JMJD3 histone demethylase, Nat. Commun. 11 (2020) 807, https://doi.org/10.1038/s41467-020-14384-z.
[10] M.C. Ramello, et al., Polyfunctional KLRG-1CD57 senescent CD4 T cells infiltrate tumors and are expanded in peripheral blood from breast cancer patients, Front. Immunol. 12 (2021) 713132, https://doi.org/10.3389/fimmu.2021.713132.
[11] J. Lian, Y. Yue, W. Yu, Y. Zhang, Immunosenescence: a key player in cancer development, J. Hematol. Oncol. 13 (2020) 151, https://doi.org/10.1186/s13045-020-00986-z.
[12] S. Rinaldi, et al., Paradoxical aging in HIV: immune senescence of B Cells is most prominent in young age, Aging 9 (2017) 1307–1325, https://doi.org/10.18632/aging.101229.
[13] Z. Liu, et al., Immunosenescence: molecular mechanisms and diseases, Signal Transduct. Targeted Ther. 8 (2023) 200, https://doi.org/10.1038/s41392-023-01451-2.
[14] B.G. Childs, et al., Senescent cells: an emerging target for diseases of ageing, Nat. Rev. Drug Discov. 16 (2017) 718–735, https://doi.org/10.1038/nrd.2017.116.
[15] S. Stekovic, et al., Alternate day fasting improves physiological and molecular markers of aging in healthy, non-obese humans, Cell Metabol. 30 (2019), https://doi.org/10.1016/j.cmet.2019.07.016.

[16] B. Lehallier, et al., Undulating changes in human plasma proteome profiles across the lifespan, Nat. Med. 25 (2019) 1843–1850, https://doi.org/10.1038/s41591-019-0673-2.
[17] J. Li, et al., Determining a multimodal aging clock in a cohort of Chinese women, Méd. 4 (2023), https://doi.org/10.1016/j.medj.2023.06.010.
[18] Z. Jia, et al., Immune-Ageing evaluation of peripheral T and NK lymphocyte subsets in Chinese healthy adults, Phenomics 3 (2023) 360–374, https://doi.org/10.1007/s43657-023-00106-0.
[19] X. Liu, J. Wu, History, applications, and challenges of immune repertoire research, Cell Biol. Toxicol. 34 (2018) 441–457, https://doi.org/10.1007/s10565-018-9426-0.
[20] Tak W. Mak, Mary E. Saunders, Bradley D. Jett (Eds.), Primer to the Immune Response, second ed., Academic Cell, 2014, pp. 111–142.
[21] J.A. Roco, et al., Class-switch recombination occurs infrequently in germinal centers, Immunity 51 (2019), https://doi.org/10.1016/j.immuni.2019.07.001.
[22] R.A. Elsner, M.J. Shlomchik, Germinal center and extrafollicular B cell responses in vaccination, immunity, and autoimmunity, Immunity 53 (2020) 1136–1150, https://doi.org/10.1016/j.immuni.2020.11.006.
[23] Q. Li, et al., Multi-omics study reveals different pathogenesis of the generation of skin lesions in SLE and IDLE patients, J. Autoimmun. 146 (2024) 103203, https://doi.org/10.1016/j.jaut.2024.103203.
[24] M.B. Lee, C.M. Hill, A. Bitto, M. Kaeberlein, Antiaging diets: separating fact from fiction, Science 374 (2021) eabe7365, https://doi.org/10.1126/science.abe7365.
[25] M.J. Wilkinson, et al., Ten-hour time-restricted eating reduces weight, blood pressure, and atherogenic lipids in patients with metabolic syndrome, Cell Metabol. 31 (2020), https://doi.org/10.1016/j.cmet.2019.11.004.
[26] J.D. Saba, Fifty years of lyase and a moment of truth: sphingosine phosphate lyase from discovery to disease, J. Lipid Res. 60 (2019) 456–463, https://doi.org/10.1194/jlr.S091181.
[27] M. Trayssac, Y.A. Hannun, L.M. Obeid, Role of sphingolipids in senescence: implication in aging and age-related diseases, J. Clin. Invest. 128 (2018) 2702–2712, https://doi.org/10.1172/JCI97949.
[28] S. Mohammed, A. Bindu, A. Viswanathan, K.B. Harikumar, Sphingosine 1-phosphate signaling during infection and immunity, Prog. Lipid Res. 92 (2023) 101251, https://doi.org/10.1016/j.plipres.2023.101251.
[29] C. Huang, et al., Gentiopicroside improves non-alcoholic steatohepatitis by activating PPARα and suppressing HIF1, Front. Pharmacol. 15 (2024) 1335814, https://doi.org/10.3389/fphar.2024.1335814.
[30] L. Ye, Y. Sun, Z. Jiang, G. Wang, L-serine, an endogenous amino acid, is a potential neuroprotective agent for neurological disease and injury, Front. Mol. Neurosci. 14 (2021) 726665, https://doi.org/10.3389/fnmol.2021.726665.
[31] T.W. Li, et al., Effects of S-adenosylmethionine and methylthioadenosine on inflammation-induced colon cancer in mice, Carcinogenesis 33 (2012) 427–435, https://doi.org/10.1093/carcin/bgr295.
[32] Y. Wang, et al., Plasma metabolic profiling analysis of gout party on acute gout arthritis rats based on UHPLC-Q-TOF/MS combined with multivariate statistical analysis, Int. J. Mol. Sci. 20 (2019), https://doi.org/10.3390/ijms20225753.
[33] N. Wu, et al., The metabolite alpha-ketobutyrate extends lifespan by promoting peroxisomal function in C. elegans, Nat. Commun. 14 (2023) 240, https://doi.org/10.1038/s41467-023-35899-1.
[34] S. Wang, et al., Phosphatidylethanolamine deficiency disrupts α-synuclein homeostasis in yeast and worm models of Parkinson disease, Proc. Natl. Acad. Sci. U.S.A. 111 (2014) E3976–E3985, https://doi.org/10.1073/pnas.1411694111.
[35] K. Lauber, et al., Apoptotic cells induce migration of phagocytes via caspase-3-mediated release of a lipid attraction signal, Cell 113 (2003) 717–730.
[36] S. Robida-Stubbs, et al., TOR signaling and rapamycin influence longevity by regulating SKN-1/Nrf and DAF-16/FoxO, Cell Metabol. 15 (2012) 713–724, https://doi.org/10.1016/j.cmet.2012.04.007.
[37] E.N. DeJong, M.G. Surette, D.M.E. Bowdish, The gut microbiota and unhealthy aging: disentangling cause from consequence, Cell Host Microbe 28 (2020) 180–189, https://doi.org/10.1016/j.chom.2020.07.013.
[38] F. Kong, F. Deng, Y. Li, J. Zhao, Identification of gut microbiome signatures associated with longevity provides a promising modulation target for healthy aging, Gut Microb. 10 (2019) 210–215, https://doi.org/10.1080/19490976.2018.1494102.
[39] K.D. Nance, et al., Cytidine acetylation yields a hypoinflammatory synthetic messenger RNA, Cell Chem. Biol. 29 (2022), https://doi.org/10.1016/j.chembiol.2021.07.003.
[40] J. Hernandez-Baixauli, et al., Alterations in metabolome and microbiome associated with an early stress stage in male wistar rats: a multi-omics approach, Int. J. Mol. Sci. 22 (2021), https://doi.org/10.3390/ijms222312931.
[41] E. Cava, N.C. Yeat, B. Mittendorfer, Preserving healthy muscle during weight loss, Adv. Nutr. 8 (2017) 511–519, https://doi.org/10.3945/an.116.014506.
[42] J. Zou, et al., CD4+ T cells memorize obesity and promote weight regain, Cell. Mol. Immunol. 15 (2018) 630–639, https://doi.org/10.1038/cmi.2017.36.
[43] N. Lian, M. Chen, Metabolic Syndrome and Skin Disease: Potential Connection and Risk, 2, 2019, pp. 89–93, https://doi.org/10.1097/01.JD9.0000559519.08557.fa.
[44] C. Xu, J. Ji, T. Su, H.-W. Wang, Z.-L. Su, The Association of Psoriasis and Obesity: Focusing on IL-17A-Related Immunological Mechanisms, 4, 2021, pp. 116–121, https://doi.org/10.1097/JD9.0000000000000155.
[45] M.J. Yousefzadeh, et al., An aged immune system drives senescence and ageing of solid organs, Nature 594 (2021) 100–105, https://doi.org/10.1038/s41586-021-03547-7.
[46] S. Borgoni, K.S. Kudryashova, K. Burka, J.P. de Magalhães, Targeting immune dysfunction in aging, Ageing Res. Rev. 70 (2021) 101410, https://doi.org/10.1016/j.arr.2021.101410.
[47] N.R. Mathew, et al., Single-cell BCR and transcriptome analysis after influenza infection reveals spatiotemporal dynamics of antigen-specific B cells, Cell Rep. 35 (2021) 109286, https://doi.org/10.1016/j.celrep.2021.109286.
[48] R.J.M. Bashford-Rogers, et al., Analysis of the B cell receptor repertoire in six immune-mediated diseases, Nature 574 (2019) 122–126, https://doi.org/10.1038/s41586-019-1595-3.
[49] M.B. Lee, C.M. Hill, A. Bitto, M. Kaeberlein, Antiaging diets: separating fact from fiction, Science 374 (2021) eabe7365, https://doi.org/10.1126/science.abe7365.
[50] E.N.C. Manoogian, L.S. Chow, P.R. Taub, B. Laferrère, S. Panda, Time-restricted eating for the prevention and management of metabolic diseases, Endocr. Rev. 43 (2022) 405–436, https://doi.org/10.1210/endrev/bnab027.
[51] M. Aoki, H. Aoki, R. Ramanathan, N.C. Hait, K. Takabe, Sphingosine-1-Phosphate signaling in immune cells and inflammation: roles and therapeutic potential, Mediat. Inflamm. 2016 (2016) 8606878, https://doi.org/10.1155/2016/8606878.
[52] A. Baeyens, et al., Monocyte-derived S1P in the lymph node regulates immune responses, Nature 592 (2021) 290–295, https://doi.org/10.1038/s41586-021-03227-6.
[53] P. Chakraborty, et al., Pro-survival lipid sphingosine-1-phosphate metabolically programs T cells to limit anti-tumor activity, Cell Rep. 28 (2019), https://doi.org/10.1016/j.celrep.2019.07.044.
[54] C. Jian, et al., Comprehensive multi-omics analysis reveals the core role of glycerophospholipid metabolism in rheumatoid arthritis development, Arthritis Res. Ther. 25 (2023) 246, https://doi.org/10.1186/s13075-023-03208-2.
[55] J. Chen, et al., Methionine-CBS axis promotes intracellular ROS levels by reprogramming serine metabolism, Faseb. J. 37 (2023) e23268, https://doi.org/10.1096/fj.202300804RRRR.
[56] M. Fassarella, et al., Gut microbiome stability and resilience: elucidating the response to perturbations in order to modulate gut health, Gut 70 (2021) 595–605, https://doi.org/10.1136/gutjnl-2020-321747.
[57] G. Bian, et al., The gut microbiota of healthy aged Chinese is similar to that of the healthy young, mSphere 2 (2017), https://doi.org/10.1128/mSphere.00327-17.
[58] S. Pang, et al., Longevity of centenarians is reflected by the gut microbiome with youth-associated signatures, Nat Aging 3 (2023) 436–449, https://doi.org/10.1038/s43587-023-00389-y.
[59] M. Rondanelli, et al., Review on microbiota and effectiveness of probiotics use in older, World J Clin Cases 3 (2015) 156–162, https://doi.org/10.12998/wjcc.v3.i2.156.
[60] H. Plovier, et al., A purified membrane protein from Akkermansia muciniphila or the pasteurized bacterium improves metabolism in obese and diabetic mice, Nat. Med. 23 (2017) 107–113, https://doi.org/10.1038/nm.4236.
[61] C. Depommier, et al., Supplementation with Akkermansia muciniphila in overweight and obese human volunteers: a proof-of-concept exploratory study, Nat. Med. 25 (2019) 1096–1103, https://doi.org/10.1038/s41591-019-0495-2.
[62] T. Tavella, et al., Elevated gut microbiome abundance of is associated with reduced visceral adipose tissue and healthier metabolic profile in Italian elderly, Gut Microb. 13 (2021), https://doi.org/10.1080/19490976.2021.1880221.
[63] S.J. Lahtinen, et al., Probiotics modulate the Bifidobacterium microbiota of elderly nursing home residents, Age 31 (2009) 59–66, https://doi.org/10.1007/s11357-008-9081-0.
[64] J. Su, et al., Remodeling of the gut microbiome during Ramadan-associated intermittent fasting, Am. J. Clin. Nutr. 113 (2021) 1332–1342, https://doi.org/10.1093/ajcn/nqaa388.
[65] H. Liu, et al., Butyrate: a double-edged sword for health? Adv. Nutr. 9 (2018) 21–29, https://doi.org/10.1093/advances/nmx009.
[66] S. Fabbiano, et al., Functional gut microbiota remodeling contributes to the caloric restriction-induced metabolic improvements, Cell Metabol. 28 (2018), https://doi.org/10.1016/j.cmet.2018.08.005.
[67] M.Y. Lim, Y.-D. Nam, Gut microbiome in healthy aging versus those associated with frailty, Gut Microb. 15 (2023) 2278225, https://doi.org/10.1080/19490976.2023.2278225.
[68] K. Yamamoto, K. Miyazaki, S. Higashi, Cholesterol sulfate alters substrate preference of matrix metalloproteinase-7 and promotes degradations of pericellular laminin-332 and fibronectin, J. Biol. Chem. 285 (2010) 28862–28873, https://doi.org/10.1074/jbc.M110.136994.
[69] M. Sun, et al., Microbiota-derived short-chain fatty acids promote Th1 cell IL-10 production to maintain intestinal homeostasis, Nat. Commun. 9 (2018) 3555, https://doi.org/10.1038/s41467-018-05901-2.
[70] J. Park, et al., Short-chain fatty acids induce both effector and regulatory T cells by suppression of histone deacetylases and regulation of the mTOR-S6K pathway, Mucosal Immunol. 8 (2015) 80–93, https://doi.org/10.1038/mi.2014.44.
[71] E.R. Mann, Y.K. Lam, H.H. Uhlig, Short-chain fatty acids: linking diet, the microbiome and immunity, Nat. Rev. Immunol. (2024), https://doi.org/10.1038/s41577-024-01014-8.
[72] L. Chen, et al., Microbiota metabolite butyrate differentially regulates Th1 and Th17 cells' differentiation and function in induction of colitis, Inflamm. Bowel Dis. 25 (2019) 1450–1461, https://doi.org/10.1093/ibd/izz046.
[73] D.C. Frankenfield, Bias and accuracy of resting metabolic rate equations in non-obese and obese adults, Clin. Nutr. 32 (2013) 976–982, https://doi.org/10.1016/j.clnu.2013.03.022.
[74] C. Wang, et al., High throughput sequencing reveals a complex pattern of dynamic interrelationships among human T cell subsets, Proc. Natl. Acad. Sci. U.S.A. 107 (2010) 1518–1523, https://doi.org/10.1073/pnas.0913939107.
[75] X. Niu, et al., Longitudinal analysis of T and B cell receptor repertoire transcripts reveal dynamic immune response in COVID-19 patients, Front. Immunol. 11 (2020) 582010, https://doi.org/10.3389/fimmu.2020.582010.

[76] S. Wiklund, et al., Visualization of GC/TOF-MS-based metabolomics data for identification of biochemically interesting compounds using OPLS class models, Anal. Chem. 80 (2008) 115–122.
[77] I. Fabijanić, D. Čavužić, A. Mandac Zubak, Meningococcal polysaccharides identification by NIR spectroscopy and chemometrics, Carbohydr. Polym. 216 (2019) 36–44, https://doi.org/10.1016/j.carbpol.2019.03.102.
[78] Z. Pang, et al., Using MetaboAnalyst 5.0 for LC-HRMS spectra processing, multi-omics integration and covariate adjustment of global metabolomics data, Nat. Protoc. 17 (2022) 1735–1761, https://doi.org/10.1038/s41596-022-00710-w.
[79] S. Sivaraj, et al., Characterization and predictive functional profiles on metagenomic 16S rRNA data of liver transplant recipients: a longitudinal study, Clin. Transplant. 36 (2022) e14534, https://doi.org/10.1111/ctr.14534.
[80] J.B. Logue, et al., Experimental insights into the importance of aquatic bacterial community composition to the degradation of dissolved organic matter, ISME J. 10 (2016) 533–545, https://doi.org/10.1038/ismej.2015.131.
[81] W. Walters, et al., Improved bacterial 16S rRNA gene (V4 and V4-5) and fungal internal transcribed spacer marker gene primers for microbial community surveys, mSystems 1 (2016).
[82] N.A. Bokulich, et al., Optimizing taxonomic classification of marker-gene amplicon sequences with QIIME 2's q2-feature-classifier plugin, Microbiome 6 (2018) 90, https://doi.org/10.1186/s40168-018-0470-z.
[83] M. Gasmi, et al., Time-restricted feeding influences immune responses without compromising muscle performance in older men, Nutrition 51–52 (2018) 29–37, https://doi.org/10.1016/j.nut.2017.12.014.